Acta Cryst. (1994). D50, 591–595

Internal Symmetry of the Molecular Chaperone cpn60 (GroEL) Determined by X-ray Crystallography

BY MICHAEL D. SPANGFORT

Department of Molecular Biophysics, Chemical Center, University of Lund, S-221 00 Lund, Sweden

BRIAN P. SURIN

CSIRO Division of Plant Industry, Canberra ACT 2601, Australia

NICHOLAS E. DIXON

Center for Molecular Structure and Function, Research School of Chemistry, Australian National University, Canberra ACT 2601, Australia

AND L. ANDERS SVENSSON

Department of Biochemistry, Chemical Center, University of Lund, S-221 00 Lund, Sweden

(*Received* 10 *September* 1993; *accepted* 20 *December* 1993)

Abstract

The *Escherichia coli* molecular chaperone cpn60 oligomer, $[cpn60]_{14}$, also called GroEL, has been crystallized and examined by X-ray crystallography and self-rotation function calculations. The crystals show unit-cell dimensions $a = 143.3$, $b = 154.6$ and $c = 265$ Å, with $\alpha = 82$, $\beta = 95$ and $\gamma = 107°$. The space group is $P1$ and crystals diffract to 7 Å. X-ray analysis shows that the oligomer has one sevenfold symmetry axis and seven twofold axes that are all perpendicular to the sevenfold. The symmetry suggests that $[cpn60]_{24}$ consists of two heptamers, $[cpn60]_7$, stacked on top of each other. The orientations of the symmetry axes of the two independent $[cpn60]_{14}$ oligomers in the triclinic unit cell have been determined relative to the crystallographic axes. The two oligomers in the unit cell are arranged side-by-side, but the second oligomer is rotated 26° around the sevenfold axis relative to the first oligomer.

Introduction

Escherichia coli $[cpn60]_{14}$ (GroEL) is a molecular chaperone that mediates the folding of certain other proteins without being part of their final structure (Ellis & van der Vies, 1991; Hartl, Martin & Neupert, 1992). The molecular mechanism for its action is still unclear to a large extent and a three-dimensional structure of $[cpn60]_{14}$ is not yet available. $[cpn60]_{14}$ is an oligomeric complex (> 800 kDa) consisting of 14 identical subunits, each with a molecular mass of 57.2 kDa (Hemmingsen *et al.*, 1988). Electron microscopic analysis of negatively stained oligomeric $[cpn60]_{14}$ (Hohn, Hohn, Engel, Wurtz & Smith, 1979; Hendrix, 1979; Ishii, Taguchi, Sumi & Yoshida, 1992) shows that the protein has an overall cylindrical shape with a central cavity which is believed to be the site for substrate binding (Langer, Pfeifer, Martin, Baumeister & Hartl, 1992; Saibil & Wood, 1993). The height and diameter of the cylinder are both around 130 Å. The 14 subunits in the oligomeric $[cpn60]_{14}$ complex are arranged in two heptameric rings, $[cpn60]_7$, which are stacked on top of each other. Crystals of $[cpn60]_{14}$ diffracting to 7 Å resolution have recently been obtained (Spangfort *et al.*, 1993) and here we report on the internal symmetry of $[cpn60]_{14}$ as revealed by X-ray crystallography and self-rotation function calculations.

Material and methods

The $[cpn60]_{14}$ protein was isolated from a recombinant *E. coli* strain containing a plasmid, pBS559, with the *groE* operon downstream of tandem bacteriophage λ promoters. For purification of $[cpn60]_{14}$, cells were grown at 303 K followed by treatment at 315 K for 3–4 h. Cells were lysed and $[cpn60]_{14}$ was isolated by ammonium sulfate fractionation and chromatography on columns of DEAE–Sephacel and Bio-Gel-A-1.5 m (Hartmann, Surin, Dixon, Hoogenraad & Höj, 1993). The purity of the protein preparation and crystals was analysed by sodium dodecyl sulfate polyacrylamide gel electrophoresis (SDS–PAGE), native PAGE and electron microscopy of samples negatively stained with uranyl acetate. Crystals were grown in a PEG 8000

©1994 International Union of Crystallography
Printed in Great Britain – all rights reserved

Table 1. *R_{merge} on intensities and completeness for the combined data set in intervals of resolution*

Cut-off data with $I <$ cut-off $\times \sigma(I)$ are not used in the statistics of completeness.

High resolution limit (Å)	No. of reflections Observed	Unique	Completeness (%) Cut-off 0.0	Cut-off 3.0	*R* factor $\Sigma\Delta I/\langle I\rangle$
17.9	4708	1742	86.8	80.0	7.9
12.7	10206	3552	96.5	85.9	9.4
10.4	13067	4626	97.4	83.1	11.2
8.9	8879	4267	71.9	54.5	14.2
Total	36860	14187	86.8	72.9	10.7

solution and analyzed using a Rigaku RU 200BEH rotating Cu-anode X-ray generator. A crystallographic data set was collected to a resolution of 8.9 Å. Measurements from five different $[cpn60]_{14}$ crystals were combined. Completeness and R_{merge} statistics of the data set are given in Table 1. Data were integrated by the program *XDS* (Kabsch, 1988*a*,*b*), and *XSCALE* (Kabsch, 1992) was used for scaling. Search of non-crystallographic symmetry with the self-rotation function method was performed with the program package *MERLOT* (Fitzgerald, 1988). The fast rotation function method of Crowther (1972) was used. Data with $F_{obs} < 3\sigma(F_{obs})$ were omitted in the calculations and the structure factors were modified to remove the Patterson origin peak. The program system *CCP4* (SERC Daresbury Laboratory, 1979) was used for production of native Patterson maps.

Results

The crystals belonged to the triclinic space group *P*1 with cell dimensions $a = 143.3$, $b = 154.6$ and $c = 265$ Å, and $\alpha = 82.4$, $\beta = 95.4$ and $\gamma = 107.3°$. The crystals contain two $[cpn60]_{14}$ oligomers per asymmetric unit and diffract to 7 Å resolution. The limited diffraction of the crystals can be explained by heterogeneity of the protein preparation. When washed crystals were analyzed by high-resolving SDS–PAGE, two monomeric cpn60 forms were observed (Spangfort *et al.*, 1993) and, in addition, isoelectric focusing under non-denaturing conditions showed the presence of up to ten different $[cpn60]_{14}$ isoforms. The observed heterogeneity may be due to the heat-induced phosphorylation of $[cpn60]_{14}$ as reported by Sherman & Goldberg (1992). However, we have been unable to find any traces of phosphotyrosine/theonine/serine in our protein preparation and we also find significant heterogeneity after phosphatase treatment *in vitro* and when $[cpn60]_{14}$ is isolated from cells grown at 303 and 310 K. Work is currently in progress to obtain electrophoretically pure protein preparations.

Native Patterson map calculation

In a Patterson map produced from native $[cpn60]_{14}$ diffraction data between 30.0 and 8.9 Å resolution no high peaks could be observed, indicating that there is no pure translational symmetry within the individual $[cpn60]_{14}$ oligomers nor between the two independent oligomers in the unit cell.

Self-rotation function calculations

Self-rotation function calculations were performed on the $[cpn60]_{14}$ data obtained with different resolution intervals in the range from 50 to 8.9 Å. Integration radii of 30, 38, 45, 53, 75, 100, 115 and 130 Å were tried but depending on the coupling between the radius of integration and the maximum usable resolution not all combinations could be tested.* Diffraction data with a resolution of less than 30 Å deteriorate the peaks in the plots. The highest signal-to-noise ratio appeared with data from 30.0 to 21.7 Å and from 30.0 to 19.2 Å resolution and with integration radii of 130 and 115 Å, respectively.

Fig. 1(*a*) is the plot resulting from a run of the self-rotation function calculation at $\kappa = 180°$ where twofold rotation axes will appear. Indeed, 14 unique peaks are found at about $\varphi = 15$ and 195° (a total of 28 peaks are found for a full rotation around the sphere). The ψ angles between these peaks are about 13°. In addition, perpendicular to these 14 peaks, a twofold symmetry axis is indicated at $\varphi = 105$ and $\psi = 88°$.

Self-rotation function calculations were also performed at $\kappa = 50°$ which is the section close to where peaks from any sevenfold axis will appear (51.4°). As seen in Fig. 1(*b*), one peak originating from a sevenfold axis is detected in the $\varphi = 105$ and $\psi = 88°$ direction. Moreover, when the peak height around the position $\varphi = 105$ and $\psi = 88°$ was plotted against the value of κ (see Fig. 1*c*), peaks appeared at rotations in κ of 2/7 of a revolution (103°) and 3/7 (154°). Peaks are also seen at 1/14, 3/14, 5/14 and 7/14 of a full revolution.

No other peaks of significance were found in the calculations, except when using an integration radius of 30 Å. In this case the 14 peaks on the section $\kappa = 180°$ along $\varphi = 15$ and 195° are replaced by two flat elongated peaks at $\varphi = 0$, $\psi = 5°$ and $\varphi = 195$, $\psi = 87°$, respectively. Also, the peaks seen in Fig. 1(*c*) at $\varphi = 105$ and $\psi = 88°$ and at different κ values are replaced by a maximum at about $\kappa = 180°$ (and $\kappa = 0°$) and a minimum at $\kappa = 90°$. This breakdown is probably due to the fact that only parts of the Patterson vectors generated from the individual

* The coupling between the integration radius and the maximum resolution in *MERLOT* Version 2.4 (Fitzgerald, 1988) is $(2.0\pi IR)/MR < 37.6785$, where IR = integration radius in Å and MR = maximum resolution in Å.

monomers are found inside the 30 Å radius. In addition, the number of vectors from all monomers with different orientations will be large around the Patterson origin. These two reasons will probably cause the low signal-to-noise ratio that is observed when using a short integration radius in the self-rotation calculations. To resolve the symmetry of the whole $[cpn60]_{14}$ oligomer an integration radius larger than 30 Å is needed in order to include vectors generated between monomers.

At the maximum radius used in our calculations, 130 Å, peaks could arise from crystal packing. However, this can only be a minor part of the symmetry observed since the results of the calculations are consistent within a radius of 38 to 130 Å. Thus, we believe that the peaks seen in Fig. 1 arise from the true internal symmetry of the $[cpn60]_{14}$ oligomer and the symmetry between the two independent oligomers in the unit cell.

Arrangement of heptamers

An important question is how the two $[cpn60]_7$ heptamers are arranged with respect to each other in the $[cpn60]_{14}$ oligomeric complex. A head-to-head arrangement will give the $[cpn60]_{14}$ oligomer a D_7 point-group symmetry according to Schoenflies nomenclature (*International Tables for Crystallography*, 1989, Vol. A). Such point-group symmetry is characterized by one sevenfold axis perpendicular to seven twofold axes. An object with a D_7 point-group symmetry will give rise to peaks at the κ sections 1/7, 2/7 and 3/7 of a full revolution. At the section $\kappa = 180°$ the seven unique twofold axes would be seen perpendicular to the sevenfold axis.

Test calculations (not shown) using low-resolution data demonstrate, however, that the true D_7 symmetry peaks are accompanied by peaks with somewhat

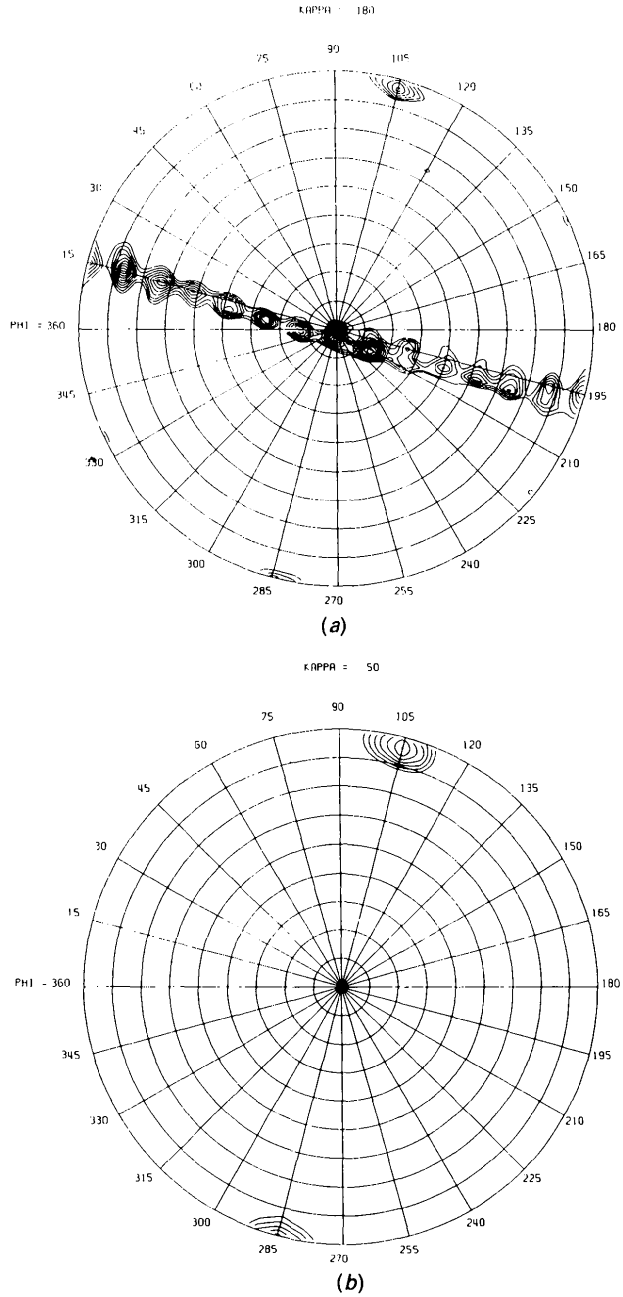

Fig. 1. (*a*) A plot of the results of self-rotation function calculation at the section $\kappa = 180°$. X-ray crystallographic data extending from 30.0 to 19.2 Å and a Patterson cut-off radius of 115 Å were used. The plot represents a half-sphere where a rotation axis, in this case a twofold axis ($\kappa = 180°$), has been applied at different longitudinal (φ) and latitudinal (ψ) co-ordinates. The crytallographic *c* axis is coming up along $\psi = 0.0°$ (the south–north pole) while the *b* axis is along $\varphi = 90$ and $\psi = 83°$ and the *a* axis along $\varphi = 197$ and $\psi = 96°$. Contouring starts at 2.0 times the root-mean-square value of the map and the interval is 0.5. (*b*) A plot of the $\kappa = 50°$ section. Data used for the calculations are the same as in (*a*). (*c*) A plot of the peak height at $\varphi = 105$ and $\psi = 88°$ as a function of κ. The peak height at $\kappa = 0°$ (no rotation of the second Patterson function) is put to 100. Resolution of the data and integration radius for the calculations are the same as in (*a*).

lower height. These additional peaks arise from Patterson vectors for subunits that are falling on top of each other but do not have the same orientation. Such additional peaks appear in the same direction as for the sevenfold axis at κ values 1/14 of a full revolution, 3/14 and so on. At the $\kappa = 180°$ section seven additional peaks are interposed between the peaks arising from the true seven twofold axes.

The peaks seen in Fig. 1 agree with the expected D_7 pattern described above. This argues in favour of $[cpn60]_7$ heptamers arranged in a head-to-head fashion in the $[cpn60]_{14}$ oligomer. A discrepancy between the predicted and our observed data is that all peaks seen in Figs. 1(*a*) and 1(*c*) have approximately the same heights. This inconsistency can be explained from the orientation of the indepenent second $[cpn60]_{14}$ oligomer as will be described below.

The sevenfold axes of the two independent $[cpn60]_{14}$ oligomers must be almost parallel in the crystallographic unit cell since a second oligomer with a different orientation of the sevenfold axis than the first oligomer would give rise to a peak at different φ and ψ coordinates in the $\kappa = 50°$ section. In addition, a second row of 14 peaks, perpendicular to the sevenfold axis of the second oligomer, would be seen at $\kappa = 180°$. As this cannot be observed in Figs. 1(*a*) or 1(*b*), it can be concluded that the oligomers are arranged in parallel with very similar orientation of their respective sevenfold axes. However, the Patterson map interpretation shows that the oligomers are not related to each other by a simple translation. An explanation of the lack of a large peak in the Patterson calculation could be that the second oligomer is rotated 1/14 of a revolution around its sevenfold axis compared with the first oligomer. This arrangement will result in extra symmetry around the origin of the Patterson map, arising from the superpositioning of the vectors from the two oligomers. The extra symmetry explains why the 14 peaks in the self-rotation function in Fig. 1(*a*) show the same amplitudes. The same is also valid for the peak amplitudes in Fig. 1(*c*). In addition, this type of rotation between the two oligomers results in a favourable packing arrangement, see Fig. 2.

The alternative arrangement of the $[cpn60]_7$ heptamers is head-to-tail. This would result in a C_7 point-group symmetry, characterized by only one sevenfold axis and no twofold axes. Since this is not in agreement with our observed data, we propose that the two $[cpn60]_7$ heptamers of oligomeric $[cpn60]_{14}$ are arranged in a head-to-head fashion. This means that the functional $[cpn60]_{14}$ oligomer initially has two identical surfaces available for co-factor and/or substrate interaction. Such an arrangement is also in agreement with a recent biochemical study of Langer *et al.* (1992).

Arrangement of the cpn60 oligomers in the unit cell

The orientation of the non-crystallographic symmetries found, relative to the definition of the triclinic unit cell, shows that the plane built of the seven twofold axes is approximately parallel with the plane formed by the *a* and *c* axes. The sevenfold axis is perpendicular to the plane of the twofold axes and forms an angle of 18° to the *b* axis in the unit cell. As described above, the sevenfold axis of the second oligomer is parallel to that of the first oligomer, but the plane of the twofold axes for the second oligomer is rotated 1/14 of a full rotation (could also be seen as a 1/2 rotation) around the sevenfold axis as compared with the first oligomer. These relationships between the symmetry axes of the cpn60 oligomers and the crystallographic axes reveal that the two oligomers must be 'standing side by side' in the unit cell, see Fig. 2.

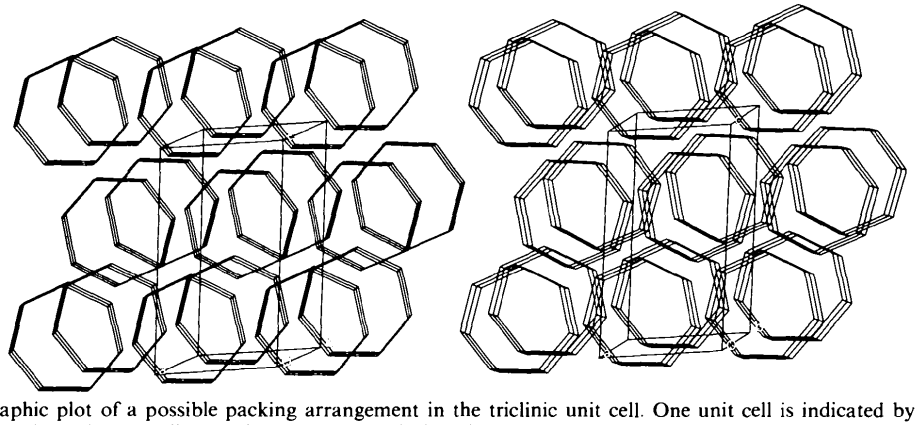

Fig. 2. A stereographic plot of a possible packing arrangement in the triclinic unit cell. One unit cell is indicated by the box with the letters a, b and c along the crystallographic axes. The origin is indicated by the letter O while the cpn60 oligomers are illustrated as seven-edged cylinders. The upper and lower rows of oligomers are crystallographically indentical while the middle row originates from the independent second oligomer. The plot was prepared with the programs *O* (Jones, Zou, Cowan & Kjeldgaard, 1991) and *PLOTAT*.

In conclusion, our X-ray analysis of $[cpn60]_{14}$ crystals shows that the $[cpn60]_{14}$ oligomer has one internal sevenfold symmetry axis arising from the assembly of seven cpn60 monomers into a $[cpn60]_7$ heptamer. Perpendicular to this sevenfold axis we observe seven twofold axes that are generated when two such $[cpn60]_7$ heptamers are stacked on top of each other in a head-to-head fashion to form a functional $[cpn60]_{14}$ oligomer. An additional twofold axis that runs parallel to the $[cpn60]_{14}$ sevenfold axis can also be resolved. This axis most likely originates from the arrangement of the two $[cpn60]_{14}$ oligomers in the crytallographic unit cell.

We wish to thank Professors A. Liljas and P.-Å. Albertsson, Drs Lars Liljas, V. Zaitsev and M. Lindahl for valuable discussions. This work was supported in parts by Carl Tryggers Stiftelse, the Swedish Research Council and by equipment funds from the SE bank, the Knut & Alice Wallenberg Foundation and the Royal Physiographical Society in Lund.

References

CROWTHER, R. A. (1972). *The Fast Rotation Function. The Molecular Replacement Method*, edited by M. G. ROSSMANN, pp. 173–185. New York: Gordon & Breach.

ELLIS, R. J. & VAN DER VIES, S. M. (1991). *Annu. Rev. Biochem.* **60**, 321–347.

FITZGERALD, P. M. D. (1988). *J. Appl. Cryst.* **21**, 273–278.

HARTL, F.-U., MARTIN, J. & NEUPERT, W. (1992). *Annu. Rev. Biophys. Biomol. Struct.* **21**, 293–322.

HARTMANN, D. J., SURIN, B. P., DIXON, N. E., HOOGENRAAD, N. J. & HÖJ, P. B. (1993). *Proc. Natl Acad. Sci. USA*, **90**, 2276–2280.

HEMMINGSEN, S. M., WOOLFORD, C., VAN DER VIES, S. M., TILLY, K., DENNIS, D. T., GEORGOPOULOS, C. P., HENDRIX, R. W. & ELLIS, R. J. (1988). *Nature (London)*, **333**, 330–334.

HENDRIX, R. W. (1979). *J. Mol. Biol.* **129**, 375–392.

HOHN, T., HOHN, B., ENGEL, A., WURTZ, M. & SMITH, P. R. (1979). *J. Mol. Biol.* **129**, 359–373.

ISHII, N., TAGUCHI, H., SUMI, M. & YOSHIDA, M. (1992). *FEBS Lett.* **299**, 169–174.

JONES, T. A., ZOU, J.-Y., COWAN, S. W. & KJELDGAARD, M. (1991). *Acta Cryst.* A**47**, 110–119.

KABSCH, W. (1988*a*). *J. Appl. Cryst.* **21**, 67–71.

KABSCH, W. (1988*b*). *J. Appl. Cryst.* **21**, 916–924.

KABSCH, W. (1992). Personal communication.

LANGER, T., PFEIFER, G., MARTIN, J., BAUMEISTER, W. & HARTL, F.-U. (1992). *EMBO J.* **11**, 4757–4765.

SAIBIL, H. & WOOD, S. (1993). *Curr. Opin. Struct. Biol.* **3**, 207–213.

SERC Daresbury Laboratory (1979). *CCP4. A Suite of Programs for Protein Crystallography*. SERC Daresbury Laboratory, Warrington WA4 4AD, England.

SHERMAN, M. Y. & GOLDBERG, A. L. (1992). *Nature (London)*, **357**, 167–169.

SPANGFORT, M. D., SURIN, B. P., OPPENTOCHT, J. E., WEIBULL, C., CARLEMALM, E., DIXON, N. E. & SVENSSON, L. A. (1993). *FEBS Lett.* **320**, 160–164.